Applied Thermal Engineering 37 (2012) 73–79

Contents lists available at SciVerse ScienceDirect

Applied Thermal Engineering

journal homepage: www.elsevier.com/locate/apthermeng

Dynamics of steam accumulation

Vladimir D. Stevanovic*, Blazenka Maslovaric, Sanja Prica

University of Belgrade, Faculty of Mechanical Engineering, Kraljice Marije 16, 11120 Belgrade, Serbia

ARTICLE INFO

Article history:
Received 15 May 2011
Accepted 4 January 2012
Available online 10 January 2012

Keywords:
Steam accumulator
Pressure transients
Numerical model

ABSTRACT

Steam accumulators are applied as buffers between steam generators and consumers in cases of different steam production and consumption rates. The steam accumulator is filled with water and steam and it operates with a sliding pressure. Dynamics of the steam accumulator charging and discharging depends on the accumulator volume, initial and boundary process parameters and condensation and evaporation rates. The non-equilibrium numerical model of steam accumulator is developed with the aim of predicting a steam accumulator capacity and as a support to the design of a control system. The model is based on the mass and energy balance equations for each phase and closure laws of phase transitions. The applied methodology is new regarding the commonly used equilibrium approach. The steam accumulator pressure transients are predicted for the case of periodic variable steam supply to a coal drying plant. The influence of the inlet steam enthalpy on the water mass and level change is investigated. The importance of the non-equilibrium evaporation and condensation modelling for the reliable prediction of steam accumulator transients is demonstrated by examples of charging and discharging tests.

1. Introduction

Steam accumulators are used in industry and power plants in order to adjust differences between steam production and consumption rates. The steam accumulator is filled with water and steam (Fig. 1). The accumulator is being charged in periods of lower steam consumption or surplus of steam production, where the pressure in the accumulator increases and the steam condenses. In periods of an increased steam consumption that is not covered with the production rate, steam is discharged to the consumer, the pressure in the accumulator decreases and water in the accumulator adiabatically evaporates. Therefore, the steam accumulator operates with sliding pressure. Without a steam accumulator, the steam generator would have to operate at a power that should provide steam for the highest consumption, while in the periods of lower consumption the excess steam would be discharged, since the steam generator usually cannot follow rapid dynamic power changes. Obviously, the application of steam accumulator substantially increases the energy efficiency of steam supply. There are numerous examples of industrial processes with periodic variable steam consumption, which require the use of steam accumulators, such as dye works in textile industry [1], glass making, rubber vulcanisation and tobacco processing [2]. In metal manufacturing the steam accumulators are used to accumulate the periodically produced steam and to supply it to industrial consumers with steady or transient steam consumption [3]. An application of the steam accumulator in an industrial boiler plant is reported in Ref. [4]. The plant supplies saturated steam to printing and dyeing mills with variable steam consumption. The steam accumulator enables economic plant operation and stabilised load levels in several time segments for a whole day. Benefits of the thermal energy storage in a steam accumulator coupled with electric boilers is analysed in Ref. [5] for an example of pulp and paper industry. The electricity is consumed for steam generation and storage during night-time hours of lower electricity price, while the accumulated steam is supplied from the accumulator to the process during day hours of higher electricity price. The steam accumulators are also used as a source of steam that performs work during a certain time period, as in case of aircraft catapulting at air carriers, or is used in the thermal power plants for the electricity production during peak loads [6]. Fast reaction times and high discharge rates make steam accumulators a promising option for compensation of fast transients in insolation for solar thermal power plants [7,8]. The application of the steam accumulator in two solar thermal power tower plants under construction in China is presented in Refs. [9,10]. The two-phase refrigerant accumulator is a key component in the automotive air conditioning system [11]. Its primary function is to store excess refrigerant mass to ensure system capacity over a large range of operating conditions.

* Corresponding author. Tel.: +381 11 3370561; fax: +381 11 3370364.
E-mail addresses: estevavl@eunet.rs, vstevanovic@mas.bg.ac.rs (V.D. Stevanovic).

1359-4311/$ – see front matter © 2012 Elsevier Ltd. All rights reserved.
doi:10.1016/j.applthermaleng.2012.01.007

Meanwhile, it captures liquid phase from the two-phase refrigerant, thus preventing damage to the compressor. Hence, its dynamical behaviour and refrigerant liquid mass storage are important for the overall cooling system performance. An influence of accumulator transients on flow instabilities of the two-phase refrigerant in a horizontal straight tube evaporator is reported in Ref. [12].

Steam pressure transients and a water level position in the accumulator depend on initial and boundary conditions, such as the initial water mass, the steam inflow and outflow rates, the inlet steam temperature and pressure (i.e. the steam enthalpy), as well as on the evaporation and condensation rates. A standard task in the steam accumulator design is to calculate its internal volume that can provide the required mass of steam accumulation or production under the accumulator pressure change between specified minimum and maximum values. Also, the task could be to calculate the steam accumulator capacity for specified volume and maximum and minimum pressure values. A more challenging task is to predict the transient pressure changes under dynamic operating conditions due to accumulator variable inlet and outlet steam flow rates and enthalpies. Despite the mature usage of steam accumulators, methods that have been used for their thermal design and for control of their operation are still approximate. The drawbacks in the current state-of-the-art of steam accumulator modelling (related to the available published models in recent years) are outlined as follows:

- In predictions of the steam accumulator volume or the accumulation and discharge capacity, the energy of phase transition removed from or added to the liquid phase is determined by using a mean value of the latent heat, which is predicted as the arithmetic mean of the latent heats at the initial and final operating pressures of the accumulator [7]. This assumption leads to approximate results; for instance, the latent heat of water varies for approximately 13% between the pressurise of 2 MPa and 5 MPa (a typical pressure span for the steam accumulator operation).
- In some models approximate equations of state for the steam phase were applied. In Ref. [3] the ideal gas law is applied although this is a very crude approximation for the saturated or close to the saturated steam state. In Ref. [7] the Antoine correlation for the relation between the saturated pressure and temperature was applied, as well as the Watson correlation for the latent heat of evaporation.
- The recent published models [3,7,8], as well as the previous ones [2,6] are based on the thermal equilibrium between the liquid and steam phase, although a substantial deviation from thermal equilibrium could exist in the accumulator during rapid charging or discharging. The equilibrium model assumes that the liquid and vapour phase in contact have the same pressure and temperature of saturation. It also implies that any thermodynamic change of the liquid and vapour state will be performed with infinite rates of evaporation or condensation. On the contrary, the models based on the thermal non-equilibrium calculate separately the liquid and vapour thermodynamic parameters, which might have different temperatures although the two phases are in contact, and the evaporation and condensation rates are finite. Application of the non-equilibrium model leads to practical implications that are important for the design of the steam accumulator, as well as for the design of a control system that should govern the accumulator transient operation. As it will be demonstrated in Section 3.4 of this paper, the non-equilibrium evaporation leads to a lower pressure in the accumulator during discharging than predicted with the equilibrium model, while the non-equilibrium condensation leads to a higher pressure during accumulator charging than predicted with the equilibrium model.

In order to overcome the drawbacks of the equilibrium steam accumulator model, the non-equilibrium model of steam accumulator operation was developed [13] with the correlations for the evaporation and condensation mass rates derived from the Herz–Knudsen equation [14]. In these correlations the value of phase transition surfaces in the steam accumulator and the local water and steam interface thermodynamic conditions are quantified with a single empirical constant.

The motivation for here presented research is a development of a new thermodynamic model of the steam accumulator, based on the thermal non-equilibrium between the liquid and vapour phase, which provides more accurate predictions of the steam accumulator pressure, temperature and water level during accumulator charging and discharging transients than the equilibrium model (still applied in the most recent research papers [3,7]). Also, the intention is to develop a model that is easily programmed for computer simulations and that can cope with complex transients of steam accumulator. The non-equilibrium model of steam accumulator is based on the mass and energy balances for each phase (liquid water and steam). The evaporation and condensation rates are calculated with empirical correlations, which take into account that the phase transition rates depend on the water mass inventory within the steam accumulator vessel. Also, the heat transfer rate from the steam towards the liquid water is calculated when steam is at a higher temperature than water. The model balance equations form a set of ordinary differential equations of the first order with pressure, masses and enthalpies of liquid and steam as dependent variables and time as independent variable. This set of equations is solved numerically with the Runge–Kutta method [15] for specified initial conditions. The model is validated by comparing numerical results with measured data from a steam accumulator charging transient. The developed model is used for an investigation of the influence of inlet steam superheating on the steam accumulator pressure transients. It is shown that the inflow of superheated steam leads to the pressure increase after charging and discharging intervals, which must be corrected by the periodic feed water charging. The presented model is a tool for the design of steam accumulator vessel volume and the control system that should govern the accumulator charging and discharging transients. It enables the prediction of steam accumulator pressure and water transients during operation. The presented model is also an improvement regarding the previously published models since it takes into account the non-equilibrium water and steam conditions in the steam accumulator and the dependence of the condensation and evaporation rates on them. Also, the necessary relations among water and steam thermo-physical parameters (such as liquid water and steam densities dependence on the pressure and temperature) are calculated with corresponding polynomials derived from the steam tables [16], while in some previous papers approximate equations of state were applied [3,7]. Compared to the results from [13] here presented model takes into account the evaporation and condensation rates dependence on the water volume in the steam accumulator and introduces the heat transfer between steam and liquid. The paper also presents the non-equilibrium effects of condensation and evaporation processes in steam accumulator transients. The importance of these effects is demonstrated by numerical simulations of steam accumulator charging and discharging tests, with a clear conclusion that these non-equilibrium effects cannot be obtained with the equilibrium steam accumulator models that represent the current state-of-the-art in the steam accumulator modelling (this is common for all recent and previously reported researches [2,3,6,7,8]).

2. Modelling approach

The steam accumulator model is based on the following balance equations

– Liquid mass balance

$$\frac{dM_1}{dt} = \dot{m}_{1B} + \dot{m}_{PT1} \quad (1)$$

– Steam mass balance

$$\frac{dM_2}{dt} = \dot{m}_{2B} + \dot{m}_{PT2} \quad (2)$$

– Liquid energy balance

$$\frac{dH_1}{dt} = (\dot{m}h)_{1B} + \dot{m}_{PT1}h'' + \dot{Q}_{21} + V_1\frac{dp}{dt} \quad (3)$$

– Steam energy balance

$$\frac{dH_2}{dt} = (\dot{m}h)_{2B} + \dot{m}_{PT2}h'' - \dot{Q}_{21} + V_2\frac{dp}{dt} \quad (4)$$

In the above equations the net mass balance of liquid water inlet and outlet flows is calculated as $\dot{m}_{1B} = \dot{m}_{1,in} - \dot{m}_{1,out}$, and consequently for the steam inlet and outlet mass flow rates $\dot{m}_{2B} = \dot{m}_{2,in} - \dot{m}_{2,out}$. These mass flow rates are prescribed time functions or depend on the difference between a calculated pressure in the steam accumulator and a prescribed pressure in the volume connected with the steam accumulator (upstream and downstream steam header, water storage reservoir, etc.). The net energy balances of inlet and outlet flows at the steam accumulator boundaries are calculated as $(\dot{m}h)_{1B} = \dot{m}_{1,in}h_{1,in} - \dot{m}_{1,out}h_{1,out}$ for liquid water and $(\dot{m}h)_{2B} = \dot{m}_{2,in}h_{2,in} - \dot{m}_{2,out}h_{2,out}$ for steam. In case of steam or water outlet flow, the outlet enthalpy equals the calculated enthalpy of the corresponding phase in the accumulator. The liquid and steam mass changes due to evaporation and condensation rates are calculated as $\dot{m}_{PT1} = \dot{m}_c - \dot{m}_e$ and $\dot{m}_{PT2} = \dot{m}_e - \dot{m}_c$. The volume balance is also applied

$$V_1 + V_2 = V \quad (5)$$

The evaporation rate is calculated as

$$\dot{m}_e = \frac{\rho_1 V_1(h_1 - h')}{\tau_e r}, \quad \text{for } h_1 > h' \quad (6)$$

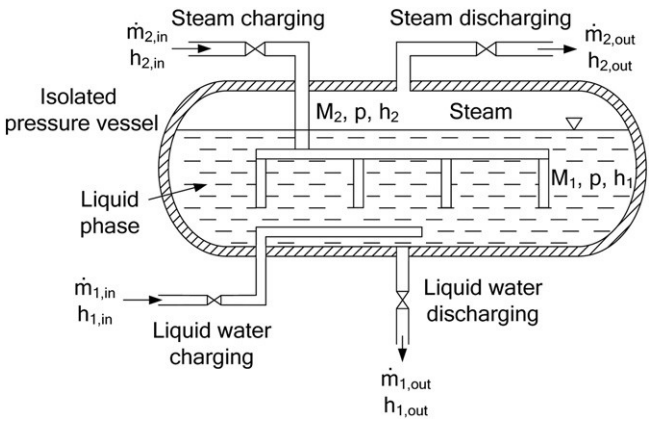

Fig. 1. Steam accumulator layout.

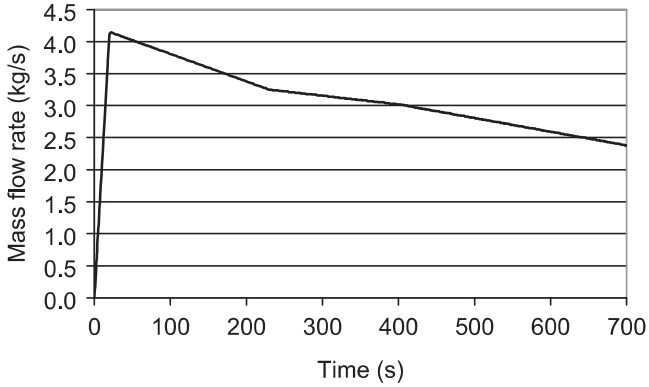

Fig. 2. Measured inlet steam mass flow rate during the test of steam accumulator charging.

and $\dot{m}_e = 0$ if water is saturated or subcooled, i.e. $h_1 \le h'$. Similarly, the condensation rate is predicted as

$$\dot{m}_c = \frac{\rho_1 V_1(h' - h_1)}{\tau_c r} \quad (7)$$

and $\dot{m}_c = 0$ if water is saturated or superheated, i.e. $h_1 \ge h'$. In (6) and (7) the evaporation and condensation relaxation times τ_e and τ_c are determined by benchmark test simulations in order to obtain good agreement of calculated and measured pressure transient values. The heat transfer rate from the superheated steam to the liquid in (3) and (4) is calculated as

$$\dot{Q}_{21} = (ha)_{21}(T_2 - T_1)V_1 \quad (8)$$

where $(ha)_{21}$ is the product of the heat transfer coefficient h and the steam–water interface area concentration a.

The system of balance Eqs. (1)–(5) is transformed in a set of first-order differential equations as presented in Appendix A. These equations are solved numerically with the Runge–Kutta method [15] for specified initial values of water and steam masses and enthalpies and initial steam accumulator pressure.

3. Results and discussions

The developed model is applied to the simulation and analyses of the steam accumulator that operates as a buffer between a steam boiler and autoclaves in a coal drying plant. The total steam

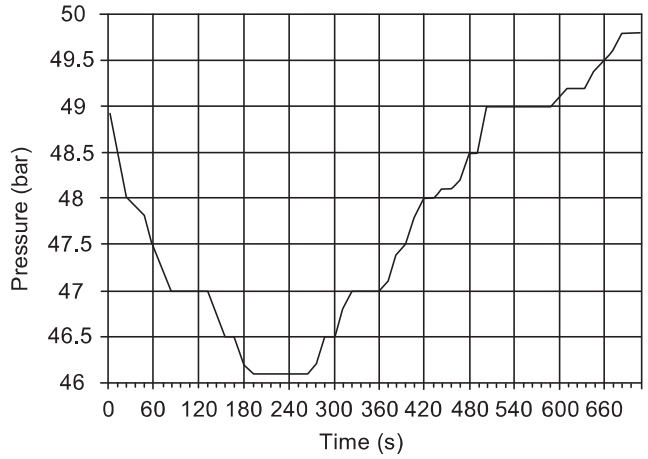

Fig. 3. Measured pressure of the inlet steam during the test of steam accumulator charging.

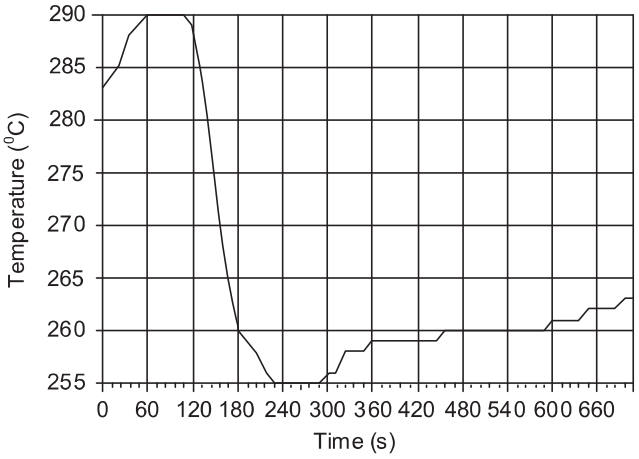

Fig. 4. Measured temperature of the inlet steam during the test of steam accumulator charging.

accumulator internal volume is 64 m^3. In all performed simulations it is assumed that in the initial state the water and steam are in thermal equilibrium determined by the initial pressure. The initial liquid water level, which determines the initial water and steam mass in the accumulator, is specified for each test.

3.1. Model validation

The developed model is validated for a test of steam accumulator charging. The measured mass flow rate, the pressure and the temperature of the inlet steam are shown in Figs. 2–4. There are no other inlet or outlet flows. The liquid water initial volume is 86% of the total accumulator volume. The calculated pressure increase is compared with the measured values in Fig. 5. A rapid pressure increase up to 36 bar is observed at the beginning of the charging process till 25 s due to the rise in the steam inlet flow rate as shown in Fig. 2. Latter on, the steady pressure increase is shown in Fig. 5. Good agreement of the calculated pressure transient with the measured data is obtained. The simulation is performed with the following values of the model empirical parameters: the condensation relaxation time is $\tau_c = 85$ s (it is assumed that $\tau_e = \tau_c$) and the product of the heat transfer coefficient from steam to liquid water and the steam–water interface area concentration is $(ha)_{21} = 5 \times 10^4$ W/(m^3 K). The evaporation and condensation relaxation times have a strong influence on the pressure change rate, and here adopted values provide good agreement between calculated and measured pressure data. The product $(ha)_{21}$ has

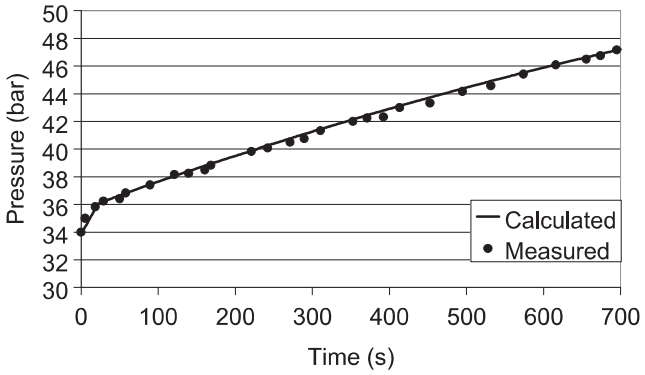

Fig. 5. Measured and calculated pressure in the steam accumulator during the test of steam accumulator charging.

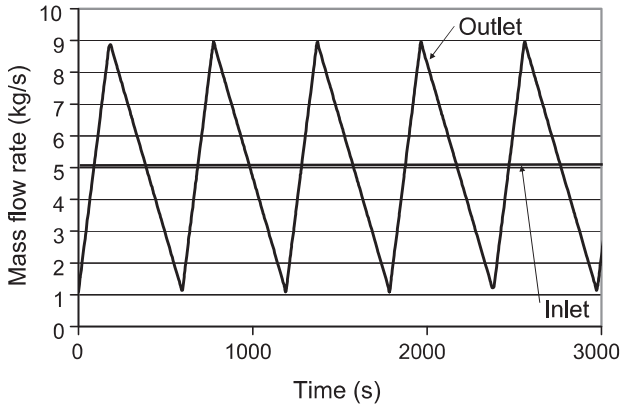

Fig. 6. Inlet and outlet steam mass flow rates at the steam accumulator that serves as a buffer between a steam boiler and a coal drying plant.

a negligible influence on the dynamics of pressure change, but it influences the steam temperature. Here adopted value of $(ha)_{21}$ leads to a difference between the steam temperature and the saturation temperature not higher than a few Celsius degrees during the course of the simulated transient.

3.2. Steam accumulator variable discharging and constant charging with saturated steam

A constant steam charging into the steam accumulator, provided by a control valve at the steam inlet, and the variable steam discharging, determined by the steam consumption in the coal drying plant and provided by a control valve at the steam outlet, are shown in Fig. 6. It is adopted that the inlet steam is saturated, which is provided by a cooling of the superheated steam from a steam boiler with a desuperheater. In the initial state the liquid water fills the half of the accumulator volume and water and steam are in thermal equilibrium at 25 bar. These conditions lead to the periodic pressure changes as shown in Fig. 7. The corresponding collapsed water level change is shown in Fig. 8. The other steam accumulator parameters, such as the liquid and steam masses, also change periodically.

3.3. Steam accumulator variable discharging and charging with superheated steam

Here analysed operating conditions of the steam accumulator are the same as presented in the previous Section 3.2, except that the superheated steam inflows into the steam accumulator, instead

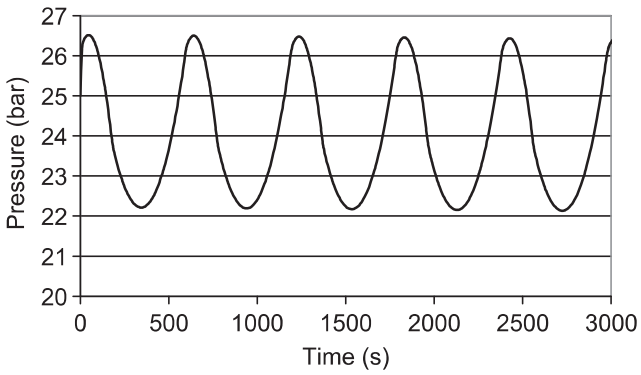

Fig. 7. Calculated pressure change in the steam accumulator that serves as a buffer between a steam boiler and a coal drying plant.

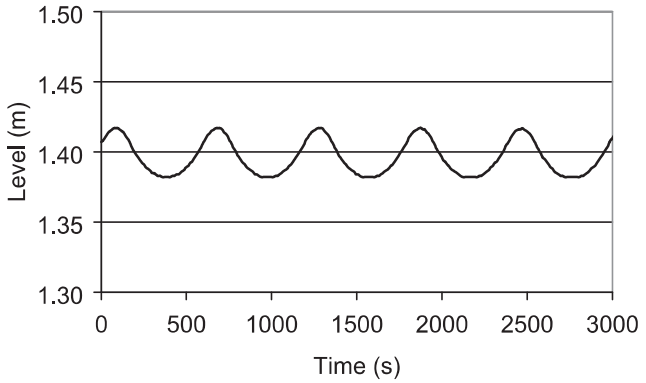

Fig. 8. Calculated water level change in the steam accumulator that serves as a buffer between a steam boiler and a coal drying plant.

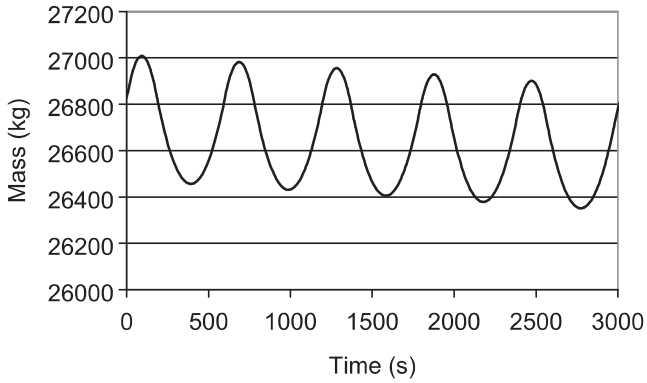

Fig. 10. Calculated liquid water mass change in the steam accumulator charged with the superheated steam.

of the saturated steam. The constant enthalpy of the inlet steam of 3000 kJ/kg is adopted, which provides a superheating of 72 °C for the initial steam pressure of 25 bar.

Compared to the results in the previous section, the mean pressure during a periodic charging and discharging steadily increases due to the inflow of superheated steam (Fig. 9). This pressure increase is caused by the water evaporation due to the excess energy of superheated steam. The decrease of water mass in the steam accumulator is shown in Fig. 10, while the steam mass increase is shown in Fig. 11. Although the mass of water in the steam accumulator decreases, the volume and the level of water slightly increase since the increase of pressure leads to the water temperature increase and the corresponding water density decrease (Fig. 12). The mean value of the pressure in the steam accumulator can be reduced by the introduction of the cold feed water. Here described phenomenon was previously reported in Ref. [2]: "If the accumulator is charged with superheated steam, more than one pound of water is evaporated per pound of steam condensed. Treated makeup water must be added. Level control should correspond to a given pressure. To avoid decreasing the available steam-storage capacity, makeup should not be added when the accumulator is discharging." This phenomenon was described almost three decades ago, but it has not been quantitatively analysed or numerically simulated previously, although it is important for the design of steam accumulator control systems.

3.4. The non-equilibrium effects of steam accumulator operation

The importance of non-equilibrium condensation and evaporation modelling is demonstrated by examples of steam accumulator charging and discharging. In both cases the initial water volume in the accumulator is 32 m^3 (the total inner volume is 64 m^3) and water and steam are in thermodynamic equilibrium in the initial state. The accumulator is charged from the initial pressure of 25 bar till the pressure of 50 bar with the constant inlet steam mass flow rate of 10 kg/s. When the pressure reaches 50 bar the inlet steam flow is stopped. The pressure change calculated with the non-equilibrium model presented in this paper is depicted in Fig. 13, together with the results of the equilibrium model that is based on the thermodynamic equilibrium between steam and water. The equilibrium model results are obtained by assuming thousand times smaller values of evaporation and condensation relaxation times τ_e and τ_c in Eqs. (6) and (7) and thousand times greater value of the heat transfer coefficient in Eq. (8) (these changes lead to thousand times greater values of mass and heat interface transfers that approximate liquid and vapour thermodynamic equilibrium conditions). Also, the same equilibrium results are obtained with the equilibrium model presented in Ref. [8]. Fig. 13 shows that the real pressure increase during the charging, predicted with the non-equilibrium model, is greater than the equilibrium pressure increase. The pressure increases up to 50 bar and after the stop of steam inflow the pressure reaches the lower equilibrium value at 45.6 bar. The equilibrium model does not predict this pressure increase for 4.4 bar over the final equilibrium state. The obtained results show that in order to charge the accumulator with the prescribed amount of steam, it is necessary to reach a higher pressure in the accumulator than a pressure predicted with the equilibrium model. This condition has to be taken into account in a design of a control system for steam accumulator operation.

In the steam accumulator discharging test, the initial pressure is 50 bar and the steam discharges with the constant mass flow rate of

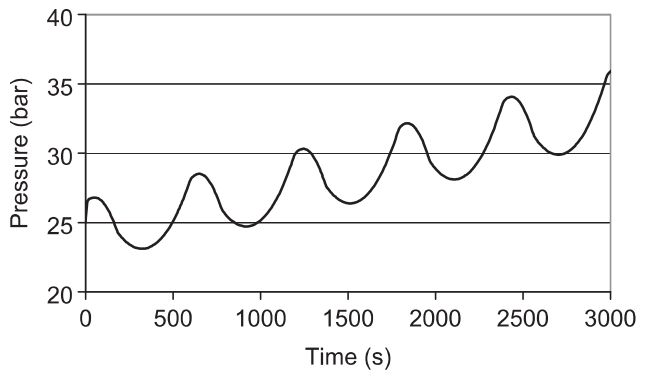

Fig. 9. Calculated pressure change in the steam accumulator charged with the superheated steam.

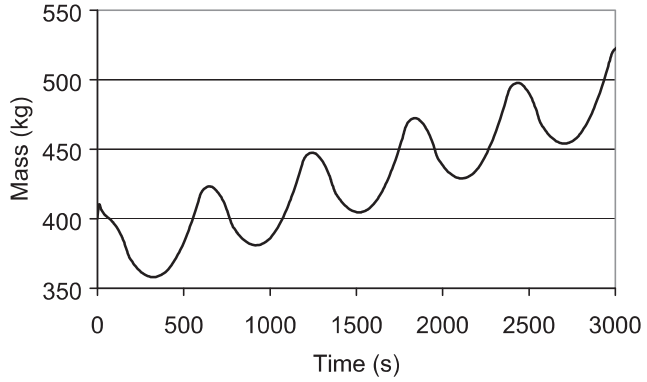

Fig. 11. Calculated steam mass change in the steam accumulator charged with the superheated steam.

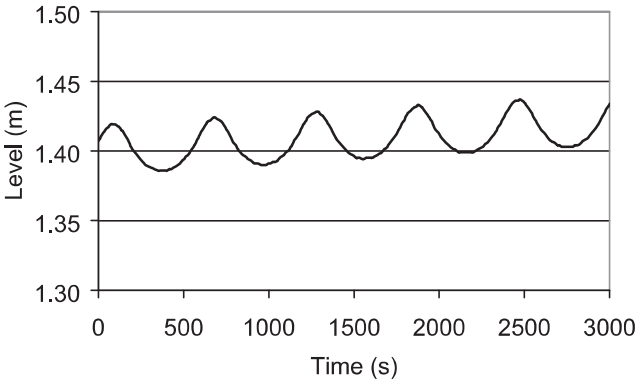

Fig. 12. Calculated water level change in the steam accumulator charged with the superheated steam.

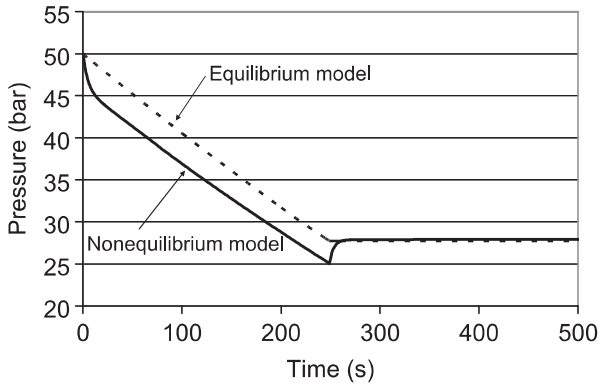

Fig. 14. Steam accumulator pressure transient during discharging – predictions with equilibrium and non-equilibrium model.

10 kg/s till the pressure of 25 bar, when its flow is stopped. The results obtained with the non-equilibrium and equilibrium models are shown in Fig. 14. The non-equilibrium model predicts the real condition with the pressure drop till 25 bar and subsequent pressure recovery to the value of 27.7 bar. The equilibrium model predicts the pressure decrease only to its final equilibrium value. Again, the equilibrium model does not provide the reliable results for the purpose of steam accumulator operation control. The final accumulator pressure is not 25 bar (the value at the instance of discharge valve closure), but a 2.7 bar higher value. The conclusion in the case of discharging transient is that in order to discharge the accumulator with the prescribed amount of steam, it is necessary to reach a lower pressure in the accumulator than a pressure predicted with the equilibrium model. Again, this transient behaviour has to be taken into account in a design of a control system for steam accumulator operation.

4. Conclusions

The numerical model for the simulation and analyses of the steam accumulator operation is developed based on the mass and energy balance equations for each phase (liquid water and steam) and non-equilibrium correlations for condensation and evaporation rates. The obtained results show changes of pressure, liquid level and water and steam masses and enthalpies. The model is validated against measured data. Performed numerical experiments show dynamic characteristics of the steam accumulator operation in cases when it is charged with saturated steam, as well as with the superheated steam. The charging with superheated steam leads to the steady increase of the accumulator mean pressure during periodic charging and discharging, which indicates a need for a subcooled feedwater injection with the aim of steam condensation and pressure reduction. Also, the non-equilibrium effects of steam accumulator operation are demonstrated with the examples of steam charging and discharging tests. It is shown that the reliable results for the design of steam accumulation control system can be obtained only by taking into account the non-equilibrium effects of evaporation and condensation, especially for accumulators that have to support fast charging and discharging rates. The important conclusion is that the use of the equilibrium steam accumulator model overpredicts pressure during accumulator discharging and underpredicts pressure during accumulator charging. A design of the control system by the predictions with the equilibrium model will lead to the false results, as demonstrated in Section 3.4. During discharging phase the lower pressure must be reached than the final equilibrium state in order to discharge the prescribed amount of steam. Also, during the charging phase, a higher pressure level must be reached than the final equilibrium pressure level in order to charge the accumulator with the prescribed steam amount. The levels of this pressure drops below final equilibrium value during discharging and the increases over final equilibrium during charging phase can be obtained only with the application of the non-equilibrium model and not with the equilibrium one.

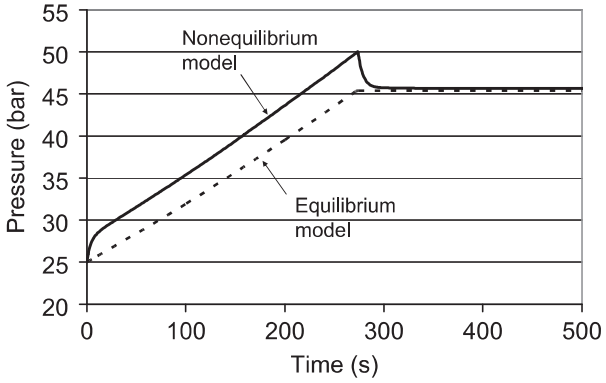

Fig. 13. Steam accumulator pressure transient during charging – predictions with equilibrium and non-equilibrium model.

Acknowledgements

This work was supported by the Ministry of Education and Science of the Republic of Serbia (Grant No. 174014).

Appendix A

The steam and liquid water volumes in the volume balance (5) are written as products of corresponding mass and specific volumes. Further, the specific volumes of liquid water and steam are written as functions of pressure and corresponding enthalpies, i.e. $v_1 = v_1(p,h_1)$ and $v_2 = v_2(p,h_2)$. The volume balance is differentiated by time and the following equation is obtained

$$v_1\frac{dM_1}{dt} + v_2\frac{dM_2}{dt} + M_1\left(\frac{\partial v_1}{\partial p}\bigg|_h\frac{dp}{dt} + \frac{\partial v_1}{\partial h}\bigg|_p\frac{dh_1}{dt}\right) + M_2\left(\frac{\partial v_2}{\partial p}\bigg|_h\frac{dp}{dt} + \frac{\partial v_2}{\partial h}\bigg|_p\frac{dh_2}{dt}\right) = 0 \quad (A.1)$$

In energy balances (3) and (4) the total enthalpies H_1 and H_2 are replaced with corresponding products of masses and specific enthalpies, and after derivation it is obtained

$$\frac{dh_1}{dt} = \frac{1}{M_1}\left[(\dot{m}h)_{1B} + \dot{m}_{PT1}h'' + \dot{Q}_{21} + M_1 v_1 \frac{dp}{dt} - h_1 \frac{dM_1}{dt}\right] \quad (A.2)$$

$$\frac{dh_2}{dt} = \frac{1}{M_2}\left[(\dot{m}h)_{2B} + \dot{m}_{PT2}h'' - \dot{Q}_{21} + M_2 v_2 \frac{dp}{dt} - h_2 \frac{dM_2}{dt}\right] \quad (A.3)$$

Substitution of (A.2) and (A.3) in (A.1) leads to

$$\frac{dp}{dt} = \frac{\left(h_1 \left.\frac{\partial v_1}{\partial h}\right|_p - v_1\right)\frac{dM_1}{dt} + \left(h_2 \left.\frac{\partial v_2}{\partial h}\right|_p - v_2\right)\frac{dM_2}{dt} - \left.\frac{\partial v_1}{\partial h}\right|_p \left[(\dot{m}h)_{1B} + \dot{m}_{PT1}h'' + \dot{Q}_{21}\right] - \left.\frac{\partial v_2}{\partial h}\right|_p \left[(\dot{m}h)_{2B} + \dot{m}_{PT2}h'' - \dot{Q}_{21}\right]}{\left(\left.\frac{\partial v_1}{\partial p}\right|_h + v_1 \left.\frac{\partial v_1}{\partial h}\right|_p\right)M_1 + \left(\left.\frac{\partial v_2}{\partial p}\right|_h + v_2 \left.\frac{\partial v_2}{\partial h}\right|_p\right)M_2} \quad (A.4)$$

Eqs. (1), (2), (A.4), (A.2) and (A.3) provide a set of five first-order ordinary differential equations for the prediction of liquid water and steam masses, steam accumulator pressure and liquid water and steam enthalpies respectively.

Nomenclature

a	steam–water interface concentration, m^2/m^3
H	total enthalpy, J
h	specific enthalpy, J/kg
h	heat transfer coefficient, $W/(m^2\,K)$
M	mass, kg
$\dot{m}$	mass flow rate, kg/s
p	pressure, Pa
$\dot{Q}$	heat transfer rate, W
r	latent heat of evaporation/condensation, J/kg
T	temperature ,K
t	time, s
V	volume, m^3
v	specific volume, m^3/kg

Greek symbols

ρ	density, kg/m^3
τ	phase change relaxation time, s

Subscripts and superscripts

B	boundary parameter
c	condensation
e	evaporation
in	inlet
PT	the phase change parameter
out	outlet
1	water
2	steam
21	interfacial transfer from steam to water
′	saturated water
″	saturated steam

References

[1] W. Goldstern, Thermal energy storage in industry and power stations, in: Proceedings of the International Conference on Energy Storage, April 29–May 1, 1981, Brighton, BHRA Fluid Engineering, pp. 113–120.
[2] N. Price, Steam accumulators provide uniform loads on boilers, Chemical Engineering 89 (23) (1982) 131–135.
[3] D.A. Shnaider, P.N. Divnich, I.E. Vakhromeev, Modeling the dynamic mode of steam accumulator, Automation and Remote Control 71 (2010) 1994–1998.
[4] J. Cao, Application of ELD and load forecast in optimal operation of industrial boiler plants equipped with thermal stores, Applied Thermal Engineering 27 (2007) 665–673.
[5] M.H. Tari, M. Soderstrom, Modelling of thermal energy storage in industrial energy systems the method development of MIND, Applied Thermal Engineering 22 (2002) 1195–1205.
[6] G. Beckmann, P.V. Gilli, Thermal Energy Storage, Springer-Verlag, Berlin, 1984.
[7] W.D. Steinmann, M. Eck, Buffer storage for direct steam generation, Solar Energy 80 (2006) 1277–1282.
[8] F. Bai, C. Xu, Performance analysis of a two-stage thermal energy storage system using concrete and steam accumulator, Applied Thermal Engineering 31 (2011) 2764–2771.
[9] E. Xu, Q. Yu, Z. Wang, C. Yang, Modeling and simulation of 1 MW DAHAN solar thermal power tower plant, Renewable Energy 36 (2011) 848–857.
[10] G.Q. Chen, Q. Yang, Y.H. Zhao, Z.F. Wang, Nonrenewable energy cost and greenhouse emissions of a 1.5 MW solar power tower plant in China, Renewable and Sustainable Energy Reviews 15 (2011) 1961–1967.
[11] B. Li, S. Peuker, P.S. Hrnjak, A.G. Alleyne, Refrigerant mass migration modeling and simulation for air conditioning systems, Applied Thermal Engineering 31 (2011) 1770–1779.
[12] N. Liang, S. Shuangquan, C. Tian, Y.Y. Yan, Two-phase flow instabilities in horizontal straight tube evaporator, Applied Thermal Engineering 31 (2011) 181–187.
[13] M. Studovic, V. Stevanovic, Non-equilibrium approach to the analysis of steam accumulator operation, Thermophysics and Aeromechanics 1 (1994) 53–60.
[14] V.P. Isachenko, V.A. Osipova, A.S. Sukomel, Heat Transfer, Mir Publishers, Moscow, 1980.
[15] R.W. Hamming, Numerical Methods for Scientists and Engineers, Dover Publications, Inc., New York, 1986.
[16] W. Wagner, H.J. Kretzschmar, International Steam Tables, Springer-Verlag, Berlin, 2007.